

Study on the Structure of Host–Guest Supramolecular Polymers

Claudia Leggio,^{†,‡} Massimiliano Anselmi,[†] Alfredo Di Nola,[†] Luciano Galantini,^{*,†,‡}
Aida Jover,[§] Francisco Meijide,[§] Nicolae Viorel Pavel,^{†,‡} Victor Hugo Soto Tellini,[§] and
José Vázquez Tato[§]

Dipartimento di Chimica, Università di Roma “La Sapienza”, P.le A. Moro 5, 00185 Roma, Italy;
Research Center SOFT-INFM-CNR, Università di Roma “La Sapienza”, P.le A. Moro 5, 00185 Roma,
Italy; and Departamento de Química Física, Facultad de Ciencias, Universidad de Santiago de
Compostela, Avda. Alfonso X El Sabio s/n, 27002 Lugo, Spain

Received March 22, 2007; Revised Manuscript Received May 22, 2007

ABSTRACT: A detailed characterization of a host–guest supramolecular copolymer, formed by adamantane and β -cyclodextrin dimers (Ad_2 and βCD_2 , respectively) in aqueous solution, has been carried out by combining small-angle X-ray scattering and light scattering experiments with molecular dynamics (MD) and Monte Carlo (MC) simulations. First, the solutions of the monomers were studied by a straightforward analysis of the scattering data. Afterward, the complex given by Ad_2 and two β -cyclodextrin molecules was investigated by correlating scattering results and MD simulations, to characterize the host–guest linkage. Finally, a detailed interpretation of the polymer scattering data was achieved by MC simulations. These simulations were performed on a single supramolecular aggregate and, in view of its peculiar shape, the complete polymer structure was considered without resorting to more general but simplified chain models. The comparison between simulations with and without excluded volume interaction points out that, at our ionic strength (sodium azide 150 mM), the polymer is close to the theta condition. Fits by reverse MC methods show that the polymer presents a shrunk conformation in solution, but it does not close in stable cyclic structures, as generally hypothesized for this kind of small oligomer. However, a polymerization degree of about 8 (4 Ad_2 and 4 βCD_2) was estimated which does not show any concentration dependence.

Introduction

The supramolecular chemistry has revived the prospect of obtaining polymers by means of reversible associations. In this framework, supramolecular polymers consist of arrays of low molecular weight molecules linked by noncovalent interactions.^{1,2} Because of the reversibility of the interactions, these polymers are in continuous equilibrium with their environment, and their properties may be adjusted by external stimuli, thus providing unique opportunities for designing tunable materials.

Ionic interactions, metal coordination, hydrogen bonding, and host–guest interactions have been exploited for the polymerization.³ In particular, host–guest supramolecular polymers, some of which show very interesting potential applications, have been obtained by using the hosting properties of cyclodextrins.^{4–18} With suitable guests these molecules give rise to very stable inclusion complexes that, when employed in the polymerization, should guarantee high polymerization degrees.² However, very often, small cyclic structures or chelate complexes seem to form which prevent the growth of large polymers.^{18–23}

Although a relevant amount of work has been addressed toward the preparation of host–guest supramolecular polymers, a complete and detailed characterization of their structure in solution is still lacking, and some aspects of the complex picture represented by the aggregation properties of these systems remain unclear. For this reason, a structural study carried out on a copolymer formed by β -cyclodextrin and adamantane dimers (βCD_2 and Ad_2 , respectively), as reported in Figure 1, is presented in this work.

Adamantyl derivatives form inclusion complexes with cyclodextrins, the interaction being highly favorable. This prefer-

ence is due to a good fit of the adamantyl group inside the β -cyclodextrin (βCD) cavity.^{6,24} For this reason, supramolecular copolymers have been recently prepared by mixing different β -cyclodextrin and adamantane dimers (Figure 1).^{16–18} Preliminary results on these systems seem to show that the polymerization degree strongly depends on the polymer flexibility, which determines the formation of closed structures, and stops the growth to small cyclic oligomers. Actually, even though very reasonable, this hypothesis lacks of definitive experimental support.¹⁸ This aspect has been also considered in our structural study.

Small-angle X-ray scattering (SAXS) and static and dynamic light scattering (SLS and DLS, respectively) have been employed. First, the single monomers have been studied to check undesired self-assembling phenomena; hence, the complex formed by Ad_2 and two βCD molecules ($\text{Ad}_2(\beta\text{CD})_2$ complex) has been investigated to characterize the host–guest interaction, and finally the copolymer has been analyzed. For a detailed description of the supramolecular structures, molecular dynamics and Monte Carlo simulations have been carried out and used for interpreting the experimental data.

Experimental Section

Materials. The Ad_2 and βCD_2 synthesis has been reported elsewhere.^{16,25} 9 wt % water was determined by thermogravimetric measurements, performed with a Netzsch STA 409 PC Luxx simultaneous thermal analyzer, on the solid samples of βCD and βCD_2 . This water fraction was considered in the preparation of the solutions. All the samples were prepared in 150 mM sodium azide in order to prevent mold growing and to guarantee some ionic concentration.

SLS and DLS Measurements. A Brookhaven instrument constituted by a BI-2030AT digital correlator with 136 channels, and a BI-200SM goniometer was used. The light source was a Uniphase solid-state laser system model 4601 operating at 532 nm. Dust was eliminated by means of a Brookhaven ultrafiltration unit

* Corresponding author: telephone (+39)-06-49913687, fax (+39)-06-490631; e-mail l.galantini@caspur.it.

[†] Dipartimento di Chimica, Università di Roma “La Sapienza”.

[‡] Research Center SOFT-INFM-CNR, Università di Roma “La Sapienza”.

[§] Universidad de Santiago de Compostela.

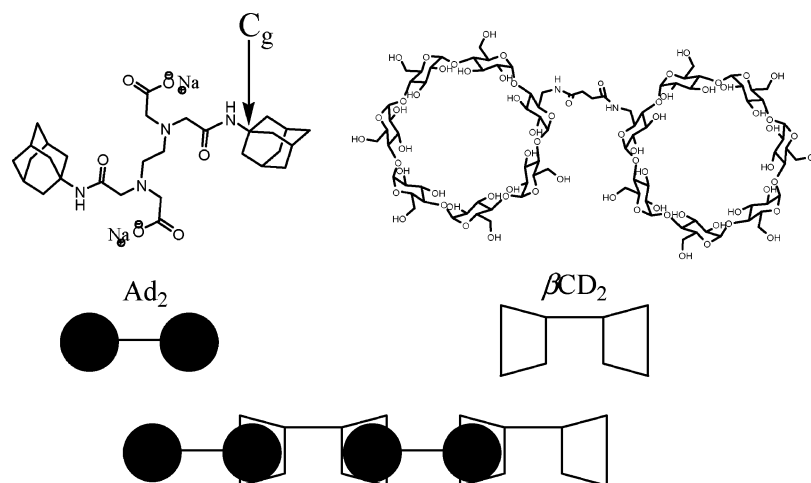


Figure 1. Structures of the precursors and schematic representation of the supramolecular polymer.

(BIUU1) for flow-through cells, the volume of the flow cell being about 1.0 cm³. Nuclepore filters with a pore size of 0.1 μm were used. The samples were placed in the cell for at least 30 min prior the measurement to allow for thermal equilibration. Their temperature was kept constant within 0.5 °C by a circulating water bath.

In the DLS experiments the intensity–intensity autocorrelation function was measured, at a particular value of the scattering vector q , and related to the normalized electric field autocorrelation function $g_1(q, \tau)$ by the Siegert relation. Therefore, $g_1(q, \tau)$ was analyzed through the cumulant expansion, and the so-called apparent diffusion coefficient D_{app} was obtained from the first cumulant by the relation

$$D_{app} = - \frac{1}{q^2} \left. \frac{d \ln g_1(q, \tau)}{d\tau} \right|_{\tau=0}$$

From this value an apparent hydrodynamic radius R_{app} was calculated by the Stokes–Einstein equation

$$R_{app} = \frac{kT}{6\pi\eta D_{app}}$$

where k is the Boltzmann constant, T is the absolute temperature, and η the solvent viscosity.

As a check, an analysis by CONTIN of $g_1(q, \tau)$ was also performed for verifying multimodal distributions.

In the SLS measurements, the $q \rightarrow 0$ limit of the excess Rayleigh ratio ΔR_θ values (ΔR_0) was analyzed by means of the equation

$$\frac{cK}{\Delta R_0} = \frac{1}{M_{app}} = \frac{1}{MS(0)} = \frac{1}{M} + 2A_2c + 3A_3c^2 + \dots \quad (1)$$

where c , M , and M_{app} are the solute concentration (g mL⁻¹), the molecular weight, and the apparent molecular weight, respectively, A_i is the i th virial coefficient, and K is a constant that depends on the solvent refractive index, the solution refractive index increment, and the laser wavelength. The measurements were performed in the range 30–150° of the scattering angle. A linear extrapolation as a function of q^2 was performed whenever an angular dependence was observed, to reach the limit value of eq 1. Otherwise, the ΔR_{90° was used. The refractive index measurements were performed by an ATAGO differential refractometer model DD7.

SAXS. The SAXS measurements were carried out in thermostated (25 ± 0.1 °C) quartz capillary of 1 mm by using a Kratky compact camera, containing a slit collimation system, equipped with a NaI scintillation counter. Ni-filtered Cu Kα radiation ($\lambda = 1.5418$ Å) was used. Scattering curves were recorded within the range $0.012 \leq q \leq 0.5$ Å⁻¹. The moving slit method was employed to measure the intensity of the primary beam. The collimated scattering intensities were put on an absolute scale, subtracted for the solvent

and the capillary contributions, and then expressed in electron units, eu (electrons² Å⁻³) per centimeter primary-beam length.^{26,27} In terms of total scattering cross section of an ensemble of particles, 1 eu corresponds to 7.94056×10^{-2} cm⁻¹.²⁸

The indirect Fourier transform method developed in the ITP program was used for interpreting the spectra.²⁹ From the desmeared $I(q)$ curve the zero angle intensity $I(0)$ is obtained and, for noninteracting particle, M can be inferred by

$$I(0) = cM\Delta\rho^2$$

where $\Delta\rho$ is the electron density difference between the particle and the solvent. If particle interactions affect the SAXS spectrum, the M_{app} value is estimated. For each sample the $\Delta\rho$ value was estimated on the basis of the molecular volumes of ref 30.

Moreover, by neglecting the particle interaction, the electron pair distribution function $p(r)$ was inferred according with the equation

$$I(q) = \int_0^\infty p(r) \frac{\sin(qr)}{qr} dr$$

The $p(r)$ function is strongly dependent on the shape and size of the scattering particles and vanishes at the maximum electron pair distance within the particle. Furthermore, it allows the determination of the electronic radius of gyration R_g .²⁹

Molecular Dynamics Simulations. MD simulations were performed with the GROMACS software package³¹ using GROMOS force field.³² The original 43A1 force field charges for cyclodextrin molecules were used, while we adopted the 53A6 force field^{33–35} for other parameters.

Atomic charges for the guest molecule (Ad_2) were obtained by the restrained electrostatic potential (RESP) methodology.^{36,37} The anionic form (deprotonated) was only considered. A total extended (all-trans) molecule geometry was used to generate the electrostatic potential at the DFT(B3LYP)/6-31G* level. Atomic charges reproducing these electrostatic potentials were obtained after consideration of the corresponding atom equivalencies due to the molecular symmetry. The molecules were solvated in a box explicit SPC/E water molecules.³⁸ Simulations were carried out at constant temperature (300 K) using the isothermal temperature coupling³⁹ within a fixed volume box and using periodic boundary conditions. The initial velocities were taken randomly from a Maxwellian distribution at 300 K, and a time step of 2 fs was used. The Lincs algorithm,⁴⁰ to constrain bond lengths, was applied. The particle mesh Ewald (PME) method⁴¹ was used for the calculation of the long-range interactions.

After a steepest descent minimization and a 100 ps MD simulation with holding the solutes fixed with positional restraints, we obtained a gradual release of the restraints on the solutes in a series of minimizations and MD steps. Finally, the productive run was performed for a total of 18 ns.

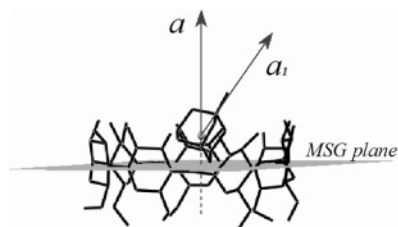


Figure 2. Reference scheme for the host–guest linkage movements in the MC simulations.

For each MD configuration, the SAXS intensities and the $p(r)$ function were estimated by a method proposed by Glatter, using the program MULTIBODY.⁴² The effective electron number for each atom, Z_{eff} , was computed by means of the relationship $Z_{\text{eff}} = Z - V\rho_s$, where Z is the atom number of electrons, ρ_s is the solvent electronic density, and V is the atomic van der Waals volume.^{30,42}

The thermodynamic calculations were performed by the multi-configuration thermodynamic integration (TI) method.⁴³ In this method, a thermodynamic coupling parameter λ is used to smoothly change the system from the initial ($\lambda = 0$) into the final ($\lambda = 1$) state and/or vice versa. In this framework, individual MD simulations are carried out at different fixed values of λ , and the averages of the derivative of the Hamiltonian with respect to λ , $\langle \partial H / \partial \lambda \rangle_\lambda$, are calculated. The free energy variation ΔG is then obtained by numerically integrating these averages from $\lambda = 0$ to $\lambda = 1$. The thermodynamic integration free energy values $\langle \partial H / \partial \lambda \rangle_\lambda$ were obtained in a stepwise manner using 21 equally spaced λ values between 0 and 1 (inclusive). Where the curvature of the integrand was large, additional λ values were used. Each MD simulation was 1 ns long with 25 ps of equilibration. In each MD simulation the solute was placed in the center of a periodic rectangular box, chosen such that the minimum distance from any solute atom to the wall was 1.5 nm. The electrostatic nonbonded interactions were evaluated using a cutoff of 1.6 nm. The standard deviation on ΔG was then calculated as

$$\sigma(\Delta G) = \left[\sum_{i=1}^{N_\lambda} \omega(\lambda_i) \sigma^2 \left(\left\langle \frac{\partial H}{\partial \lambda} \right\rangle_{\lambda_i} \right) \right]^{-1/2}$$

where N_λ is the number of points at which the ensemble average has been calculated, $\omega(\lambda_i)$ is the weight factor from the trapezoidal integration, and $\sigma \langle \partial H / \partial \lambda \rangle_{\lambda_i}$ is the error in the ensemble average.

Monte Carlo Simulations. MC simulations were performed for calculating SAXS spectra of the polymeric solutions. Starting from the structural model of the supramolecular polymer (without the hydrogens), the movements were performed by the method described by Stellman and Gans⁴⁴ around the bonds of the joining chain of the two dimers. Freely rotating torsion angles were considered for each single bond, and restriction to 0 or 180° was assumed for the rotation around the amidic C–N bond. The cyclodextrin, the adamantyl, and the carboxymethylene residues were kept rigid during the simulation. The host–guest linkage was built by fixing the adamantyl centroid on the axis (a) passing for the centroid of the cyclodextrin glycosidic oxygens and perpendicular to their mean-square plane (MSG plane). The distance between the adamantyl centroid and this plane was kept constant. Rotation around the axis (a_1) joining the centroid and the carbon atom C_g of the adamantane (Figures 1 and 2) as well as tilting movements of a_1 with respect to a were allowed in order to account for some linkage flexibility. In details, whenever a pivotal adamantyl centroid was selected, a_1 was superimposed to a by moving the shorter part of the polymer. Hence, a first rotation around a (a_1) was performed and followed by a second rotation of a randomly chosen angle (between 0 and 45°) around a random direction perpendicular to a . When the excluded-volume effect was considered, a radius of 1.2 Å was assumed for each atom and used to check intrapolymer overlaps. For each conformation of the polymer, $I(q)$ was calculated by MULTIBODY, as reported in the previous

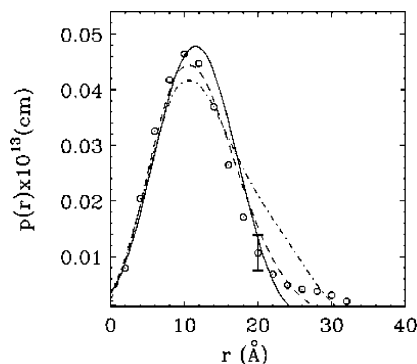


Figure 3. $p(r)$ inferred from the experimental SAXS spectrum (open circles) and calculated for the βCD_2 in different conformations corresponding to R_g values of 8.9 (full line), 9.2 (dashed line), and 10.2 Å (dot-dashed line). For clarity, only a few error bars of the observed $p(r)$ are shown.

section. Starting from the extended conformation (all trans), for each run a number of MC steps were performed for equilibrating the chain and the $I(q)$ calculation was performed on 1000 accepted conformations. The final $I(q)$ curve was averaged on the results of at least 10 different runs. The accuracy of the runs was estimated to be within 1%.

A reverse MC procedure was also used to fit the supramolecular polymer SAXS spectra. In the minimization, for each conformation, the calculated intensities were smeared by the normalized weighting functions for slit length and slit width effects and then compared with those collected by the Kratky camera. The conformations were accepted on the basis of the R value estimated as

$$R = \frac{1}{N} \sum_i \frac{(I_o(q) - I_c(q))^2}{\sigma_i^2} \quad (2)$$

where $1 \leq i \leq N$ (number of experimental points), $I_o(q)$ and $I_c(q)$ are the observed and calculated intensities, and σ_i^2 is the $I_o(q)$ variance. The details of the method are reported elsewhere.⁴⁵

In all kinds of simulations an $I(q)$ curve averaged over all the accepted configurations was estimated. From this curve a calculated $p(r)$ function was extracted by ITP.

Results and Discussion

Monomers. The light scattering and SAXS M_{app} values ($(2.1 \pm 0.2) \times 10^3$ and $(2.3 \pm 0.2) \times 10^3 \text{ g mol}^{-1}$, respectively), measured for βCD_2 10 mM solution, are very similar to the one obtained from its formula ($M = 2350 \text{ g mol}^{-1}$), thus pointing out that no self-aggregation is given by the host dimer. The experimental R_g value ($9.6 \pm 0.1 \text{ Å}$) and the $p(r)$ function are consistent with the monomeric form since they are similar to those estimated by MULTIBODY for the βCD_2 molecule in different conformations (Figure 3). Finally, a R_{app} value of $12.5 \pm 0.5 \text{ Å}$ is inferred from DLS, which is close to the R_g value.

Conversely, light scattering data on Ad_2 solutions unambiguously point out self-assembling phenomena.¹⁶ As a matter of fact, SLS measurements on Ad_2 15 mM water solution give a M_{app} value of $1.3 \times 10^4 \text{ g mol}^{-1}$, which is much higher than the Ad_2 formula weight (602 g mol^{-1}). For the same sample, the CONTIN method analysis of the DLS data provides a decay time distribution with two peaks related to apparent hydrodynamic radii of about 1 and 80 nm, probably corresponding to the Ad_2 molecule and a much bigger aggregate.

$\text{Ad}_2(\beta\text{CD})_2$ Complex. It is obvious that the Ad_2 self-association represents an undesired phenomenon which competes with the copolymerization when βCD_2 and Ad_2 are mixed. Therefore, the conditions where the supramolecular polymerization is the most favorable aggregation process must be

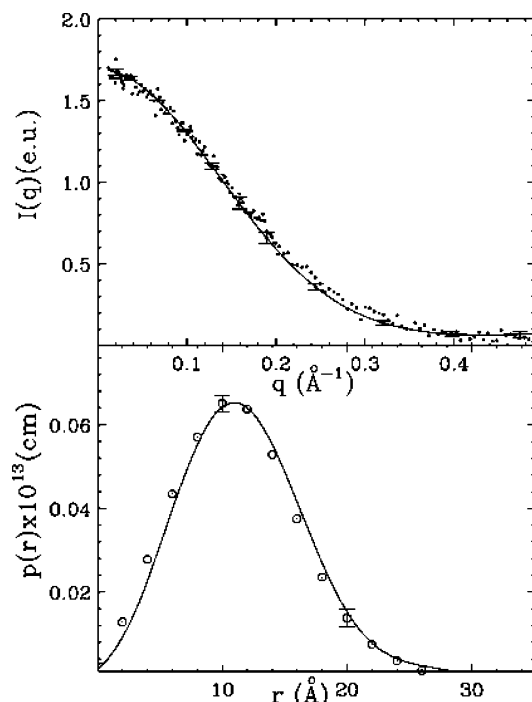


Figure 4. Experimental SAXS spectrum (dots, upper panel) and extracted $p(r)$ function (open circles, lower panel) of a solution containing Ad_2 (10 mM) and βCD (20 mM). The full lines represent the patterns obtained by the MD simulation on the $\text{Ad}_2(\beta\text{CD})_2$ complex. For clarity, only a few error bars of the MD calculated intensity and of the experimental $p(r)$ function are reported.

searched. For this purpose, light scattering and SAXS measurements on solutions containing Ad_2 and βCD with 1:2 molar ratio were performed. The results show that in these solutions the Ad_2 aggregates are disrupted because of the adamantyl- βCD complexation. In particular, light scattering M_{app} and R_{app} values of $(2.6 \pm 0.2) \times 10^3 \text{ g mol}^{-1}$ and $10.0 \pm 0.5 \text{ \AA}$ were obtained, which are consistent with the formation of an $\text{Ad}_2(\beta\text{CD})_2$ inclusion compound (formula weight 2873 g mol^{-1}). The SAXS data (Figure 4) support these results by providing $M_{\text{app}} = (2.8 \pm 0.2) \times 10^3 \text{ g mol}^{-1}$ and $R_g = 8.6 \pm 0.1 \text{ \AA}$.

In view of the supramolecular arrangement of Figure 1, it is expected that the polymer properties, such as the contour length and flexibility, are strongly affected by the structure of the host-guest linkage. Reasonably, this linkage is similar to the complex formed by the βCD and the adamantyl group in $\text{Ad}_2(\beta\text{CD})_2$. Therefore, a detailed description of this complex can be fundamental for the analysis of the polymer. On the basis of these considerations, a complete study of the $\text{Ad}_2(\beta\text{CD})_2$ structure was performed by combining MD simulation and SAXS data. The starting configurations for the simulations were built by assuming the Ad_2 molecule in a total extended (all-trans) geometry, with the adamantyl groups entering the βCD cavities by their secondary rims, and the Ad_2 principal axis perpendicular to the cyclodextrin MSG planes. Different starting structures were tested by changing the depth of penetration of the adamantyl group inside the βCD . The dynamic evolution of the $\text{Ad}_2(\beta\text{CD})_2$ complex was followed by monitoring the trajectory of the estimated gyration radius. Initially, the $\text{Ad}_2(\beta\text{CD})_2$ complex is characterized by a gyration radius of around $10.0\text{--}11.5 \text{ \AA}$, larger than the experimental radius of gyration (8.6 \AA), and reasonably due to the very extended configuration chosen for the initial coordinates. After about 2 ns, the complex reaches an equilibrium state characterized by shorter gyration radius values, in a range of about 8.4 and 9.2 \AA , in agreement with the experimental data. This final equilibrated state is

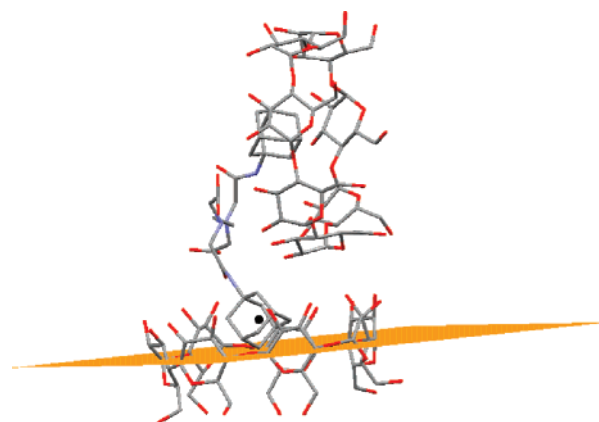


Figure 5. A typical MD configuration of the $\text{Ad}_2(\beta\text{CD})_2$ complex. In orange and black are reported a MSG plane and an adamantane centroid, respectively.

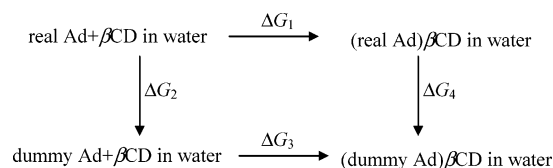
maintained for the rest of the simulation for a total period of about 15 ns. Moreover, in the entire simulation the host-guest aggregates are conserved.

From all the equilibrated configurations, the average SAXS spectrum and $p(r)$ function were estimated. The error bars were evaluated by the variations of the curves obtained from a set of 10 MD subtrajectories. As reported in Figure 4, the calculated patterns are in good agreement with the experimental curves.

The snapshots of the equilibrated $\text{Ad}_2(\beta\text{CD})_2$ complex as obtained from MD simulation show a peculiar folded structure (Figure 5). Moreover, concerning the host-guest interactions, the snapshots point out that the adamantyls penetrating inside the βCD cavities stop well before their centroids pass the MSG planes, which is in agreement with crystallographic structures of complex and supramolecular polymer formed by βCD -adamantyl group interaction.^{6,46}

These structures show that the interior of the βCD cavity is not a smooth cone or cylinder but has a constriction in the neighborhood of the glycosidic oxygens, blocking the entrance of the guest molecules. The distance between the adamantyl centroid and the MSG plane averaged on the MD configurations is $\sim 2.0 \text{ \AA}$, a reasonably shorter distance is observed in the supramolecular polymer crystal (1.15 \AA).⁶

MD simulations were also carried out for estimating the free energy of the complexation. Experimental data point out that the energies for the *one site-one site* interaction between Ad_2 or other several water-soluble adamantyl derivatives and βCD are very similar.^{16,24} This means that the polar residue bonded to the adamantyl, which is always present in these derivatives, poorly influences the host-guest interaction. Therefore, general results can be obtained by thermodynamic calculations performed on a simplified system taking into account only the adamantane and the βCD molecule. The free energy of the inclusion process was defined as the work required to transfer the guest from the cyclodextrin cavity to the solvent. This energy was not determined directly but was estimated from the thermodynamic cycle reported in the following scheme



as $\Delta G_1 = \Delta G_2 + \Delta G_3 - \Delta G_4$. In this scheme, an adamantane (Ad) that is interacting with the solvent molecules and the rest

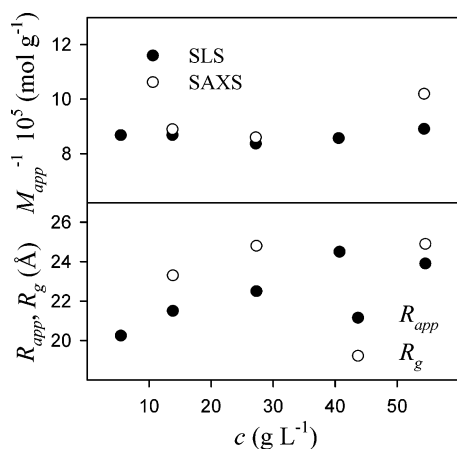


Figure 6. Some SAXS and LS parameters of polymeric solutions as a function of the polymer concentration c .

Table 1. LS and SAXS Parameters of Polymeric Samples as a Function of Polymer Concentration^a

c (g L ⁻¹)	LS		SAXS	
	R_{app} (Å)	M_{app} (10 ³ g mol ⁻¹)	R_g (Å)	M_{app} (10 ³ g mol ⁻¹)
5.43	20.3	11.7		
13.8	21.5	11.7	23.3	11.4
27.3	22.5	11.8	24.8	11.7
40.7	24.5	11.7		
54.5	23.9	11.4	24.9	9.80

^a Esd's are within 0.3 Å (R_{app} , R_g) and within 3×10^2 g mol⁻¹ (M_{app}).

of the system is in the real state. When its nonbonded interactions with the solvent molecules and the rest of the system are switched off, it is in the dummy state. Thus, ΔG_2 is the work required to transform the real adamantane into a dummy adamantane in water while ΔG_3 is the work to transfer the dummy adamantane from the solvent to the β CD cavity. Because all the interactions between the dummy adamantane and the rest of the system are removed, $\Delta G_3 = 0$. Finally, ΔG_4 is the work required to transform the adamantane from real to dummy in water inside the cyclodextrin cavity.

The calculation of each ΔG_n ($n = 2, 4$) term by MD simulation was straightforward by using the multiconfiguration TI method. A ΔG_1 value of -33 ± 2 kJ mol⁻¹ was estimated, in agreement with the experimental data reported in literature, mainly distributed within the range -33 to -22 kJ mol⁻¹.^{16,24,47}

Polymer. Polymeric solutions were prepared by mixing equimolar amount of Ad₂ and β CD₂. Some SAXS and light scattering parameters of these solutions as a function of concentration are reported in Figure 6 and Table 1. Published results point out that a concentration induced polymer growth is sometimes observed for this kind of systems. However, being affected by interparticle interaction, the apparent quantity of Figure 6 could mask this growth.

As shown in Figure 6, the SAXS spectra were collected up to a quite low concentration (13.8 g L⁻¹). Reasonably, at this dilution, the effect of interchain interactions on the $I(q)$ curve is negligible, thus allowing an interpretation on the basis of a single chain scattering function.

Model expressions for the scattering functions of semiflexible worm chains with and without excluded-volume interaction, and with a finite cross section, are available in the literature, which should represent polymer spectra in theta and good solvent, respectively.^{48,49} These expressions were used for fitting the SAXS curve of the most diluted sample, but unsatisfactory

minimizations were obtained even when some polydispersity was taken into account.⁵⁰ A possible explanation of this result is that our polymer does not fit the basic interaction model of these equations. Moreover, we must remember that the peculiar shape of our supramolecular array, which is a kind of balls and chains sequence (Figure 1), is significantly different from the worm structure of homogeneous thickness represented by the mentioned expressions. Because of these problems, MC simulations were performed on the complete structure of our polymer and used for interpreting the SAXS intensities, thus trying to achieve a detailed characterization of the supramolecular chain. The starting structure was built assuming the cyclodextrin and the adamantyl group as observed in the crystal of ref 6. The linkage was realized by placing the adamantane with its centroid at 2 Å from the MSG plane, in agreement with the above-mentioned MD results. A chain of four Ad₂- β CD₂ repetitive units was considered, in agreement with the SAXS and SLS averaged M_{app} value ($(11.6 \pm 0.3) \times 10^3$ g mol⁻¹).

As shown in Figure 7, the curve calculated by MC simulation assuming excluded-volume interactions (MC_{ex} simulation) does not fit the experimental data. However, a much better agreement between calculated and experimental patterns is obtained when the interactions are neglected (MC_i simulation). These results point out that in, our conditions, the aqueous medium does not represent a good solvent for the polymer that hardly assumes the most extended conformations.

On the basis of the ΔG_1 value estimated by MD simulations, and assuming free monomers in equilibrium with the complex, a constant of 6.1×10^5 , for the host guest linkage formation, is calculated. According to this value and to an isodesmic polymerization process, the weight-averaged polymerization degrees (number of polymerized Ad₂ or β CD₂ molecules) should vary roughly from 70 to 220 in the analyzed concentration range (5.4–54.5 g L⁻¹).^{2,51} In view of these considerations, the results of Figure 6 unambiguously point out that our polymer does not show this expected growth. In particular, by assuming a negligible second virial coefficient A_2 value in eq 1, which is reasonable in view of the results inferred from the simulated spectra, the observed $1/M_{app}$ patterns of Figure 6 point out that polymer size remains roughly constant.

According to the results exposed so far, the $p(r)$ functions extracted from SAXS spectra at different concentrations are very similar, which means that the polymer sizes does not change and that the scattering data are roughly unaffected by interactions (Figure 7).

To get information on the most probable conformations of the polymer in solution, a reverse MC minimization, including the excluded-volume interactions (RMC_{ex} simulation), was also carried out. An excellent fit is achieved with this method (Figure 7). The analysis of the best fitting conformations shows that the polymer in solution is quite shrunk (Figure 8), as expected in view of the solvent quality.

Being related to the chain conformation, the SAXS spectra allow also to check the formation of cyclic or close to cyclic structures which are generally hypothesized for this kind of not growing supramolecular polymers.¹⁸ In the frame of our fitting procedure, this check can be performed by MC simulations restricted to cyclic polymer conformations. In an off-lattice simulation, this restriction is imposed by selecting the fraction of conformations with end separation less than a limit value.⁵² This principle was followed in a reverse MC minimization (RMC_{excy} simulation) of our reference spectrum. The excluded volume interactions were taken into account, and the limit was imposed to the distance between the centroids of the terminal

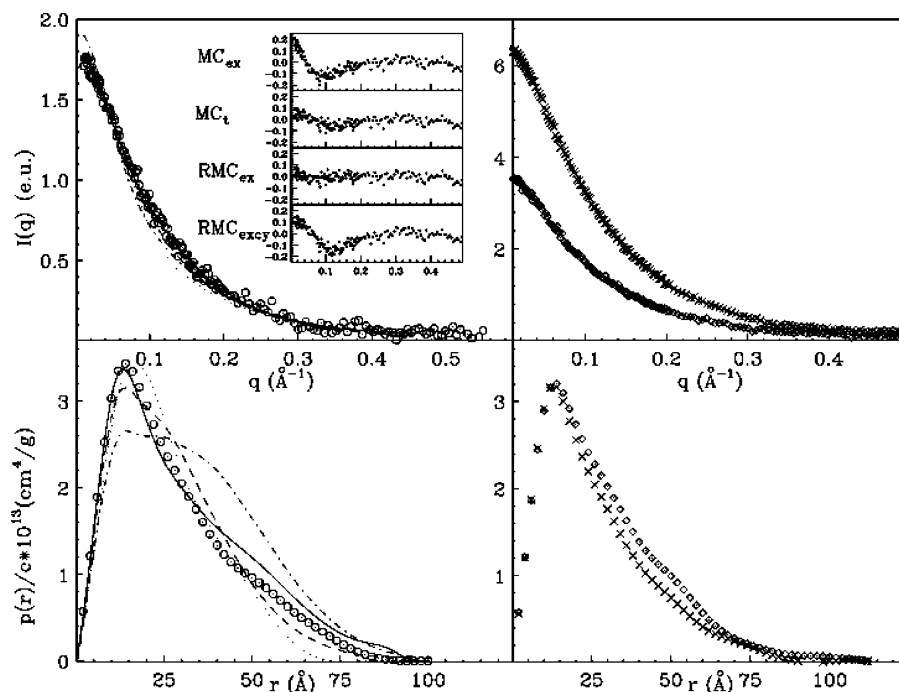


Figure 7. SAXS experimental spectra and extracted $p(r)$ functions of polymeric solution at polymer concentrations of 13.8 (open circle, left panels), 27.3 (open diamond, right panels), and 54.5 g L⁻¹ (cross, right panels). The estimated patterns are reported for MC_t (dashed line), MC_{ex} (dot dashed line), RMC_{ex} (full line), and RMC_{excy} simulations (dotted line), described in the text. The intensity residuals are reported in the insets. The R values calculated as in eq 2 are 0.227 (MC_{ex}), 0.131 (MC_t), 0.088 (RMC_{ex}), and 0.250 (RMC_{excy}).

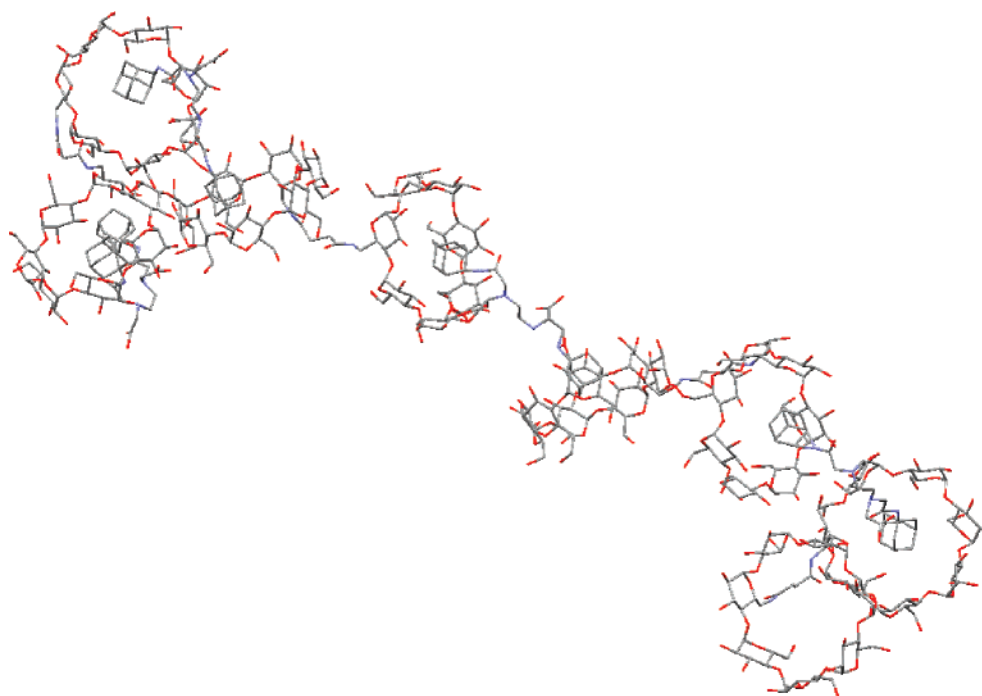


Figure 8. Best fitting conformation inferred from the RMC_{ex} simulation.

adamantane and of the cyclodextrin glycosidic oxygens. With a limit distance ≤ 5 Å, no accepted conformation was obtained in 10^6 attempts, which means that the cyclic structure is practically impossible for our chain. Therefore, a value of 8 Å was used to get a satisfactory statistic. The sampling of cyclic structure in the simulations is testified by some accepted conformations reported in the Supporting Information. As reported in Figure 7, the obtained best fitting curve and the experimental data are significantly different, thus testifying that cyclic structures are hardly formed by the polymer. Since the restraints imposed by the rigidity of the carboxy methylenic

residues could affect this result, the same reverse MC minimization was performed by eliminating the carboxylic groups in the overlap check. As reported in the Supporting Information, the fit does not improve significantly.

This conclusion throws some doubt on the hypothesis that cyclization is responsible for the stop of the polymer growth. However, our results highlight an alternative explanation to the observed behavior. As previously stated, conformations not very extended, with some globular parts, are assumed by the polymer (Figure 8) because of the solvent quality. We suggest that the coiled moieties can trap the terminal adamantyl, thus removing

it from the interaction with the β -cyclodextrin and then stopping the polymer growth. As well as the previously hypothesized cyclization, this situation can take place at a peculiar polymer length, which is shorter the more flexible the supramolecular chain, in agreement with results reported in literature.¹⁸ On the basis of the cyclization mechanism of termination, the search of long polymers was addressed toward the preparation of rigid dimers, in order to realize more rigid polymers unable of closing in cycles.¹⁸ Actually, our results point out that large polymers could be prepared by improving the solvent quality, to avoid the formation of intrachain hydrophobic moieties. This could be done, for example, by using a more hydrophobic solvent. However, being the host–guest linkage formed by hydrophobic interactions, the preparation of these polymers in nonaqueous medium is unadvisable. Conversely, without affecting the linkage strength, the polymer solvation can be modulated by changing the properties of the joining chains of the β -cyclodextrin and adamantane dimers. Some recent results on this kind of polymers support our conclusions. In particular, they show that the polymers formed by dimers with more flexible but also more hydrophilic joining chains are bigger than those given by dimers with joining chains more rigid but also more hydrophobic.^{17,18}

To check the influence of stoichiometric errors in the preparation of polymeric solutions, scattering data on polymer samples with 10% or 20% molar excess of β CD₂ or Ad₂, respectively, were collected. As reported in the SI no sensitive variation of the LS and SAXS results were observed with the β CD₂ excess. Conversely, in the case of the Ad₂ excess, a bimodal distribution of the hydrodynamic radii was inferred by the CONTIN analysis of the DLS data, with the two peaks corresponding to the hydrodynamic radii of the polymer (~2 nm) and the Ad₂ aggregate (~120 nm). However, no influence of the Ad₂ aggregate was observed on the structural information inferred from the SAXS spectra, which remain very similar to those reported above (Supporting Information). These results point out that the formed host guest oligomer is quite stable and practically unaffected by slight excess of one of the two dimers.

It is important to remark, finally, that the self-association of the Ad₂ dimer could also sensitively affect the polymer growth. In fact, it removes free Ad₂ from the solution, thus competing with the polymerization. Even though no big Ad₂ aggregates were observed in the polymeric solutions containing equimolar amounts of the two dimers, the presence of a small amount of Ad₂ oligomers (dimers, trimers, and so on), whose contribution to the scattering data is negligible, cannot be completely ruled out. If present, this aggregation could also contribute to the stop of the polymer growth and could explain some of the results so far reported in literature. However, in our previous paper, we observed that the same Ad₂ dimer give rise to bigger supramolecular polymer or to dendrimers which grow with the concentration when polymerizes with a more rigid β -cyclodextrin dimer or with a β -cyclodextrin trimer, respectively.¹⁶ All these results indicate that, despite the possible influence of the Ad₂ aggregation, the conformation of the polymer significantly affects its growth, thus supporting our conclusions based on the polymer structure.

Conclusions

A detailed structural study was carried out, by combining SAXS and light scattering experiments with MD and MC simulations, on a short host–guest supramolecular copolymer formed by adamantane and β -cyclodextrin dimers in aqueous

solution. After a preliminary analysis of the solutions of the monomers, the complex given by the adamantane dimer and two β -cyclodextrin molecules was investigated, by the scattering techniques and MD simulations, to characterize the host–guest linkage. Afterward, with this information, a detailed interpretation of the polymer SAXS curve was achieved by MC methods. The simulations were performed on the complete polymer structure without resorting to more general but simplified chain models, which are far from representing the peculiar shape of the supramolecular polymer. The results show that, at our ionic strength, the polymer is close to the theta condition, thus assuming a shrunk conformation in solution and avoiding the polymer growth. Conversely, it does not close in stable cyclic structures that are normally invoked to justify their low polymerization degree. Assuming negligible interchain interactions, the scattering results show that the polymerization degree stops at a value of about 8 (4 Ad₂ and 4 β CD₂) and does not depend on the concentration.

Acknowledgment. Thanks to Professors Vittorio Crescenzi and Edoardo Giglio for valuable discussions and to Dr. Alessandro Latini for the thermogravimetric measurements. We are also thankful for the Spain-Italy Integrated Action grants. The authors from USC thank the Ministerio de Ciencia y Tecnología (Project MAT2004-04606) and Xunta de Galicia (PGIDIT05PXIC26201PN) for financial support. The authors from “La Sapienza” thank the MIUR for financial support (FIRB project RBIN04PWNC and PRIN 2006).

Supporting Information Available: RMC_{excy} minimization of the polymer SAXS spectrum at $c = 13.8 \text{ g L}^{-1}$ without considering the carboxylic groups in the overlap check (Figure 1S); some accepted conformations sampled by RMC_{excy} simulations (Figure 2S); and $p(r)$ functions for the spectra of polymeric samples with 1:1, 1.2:1, and 1:1.1 Ad₂: β CD₂ molar ratios (Figure 3S). This material is available free of charge via the Internet at <http://pubs.acs.org>.

References and Notes

- (1) Ciferri, A. *Macromol. Rapid Commun.* **2002**, *23*, 511.
- (2) Ciferri, A., Ed. *Supramolecular Polymers*, 2nd ed.; Taylor & Francis: New York, 2005.
- (3) Brunsvel, L.; Folmer, B. J. B.; Meijer, E. W.; Sijbesma, R. P. *Chem. Rev.* **2001**, *101*, 4071.
- (4) Hirotsu, K.; Higuchi, T.; Fujita, K.; Ueda, T.; Shinoda, A.; Imoto, T.; Tabushi, I. *J. Org. Chem.* **1982**, *47*, 1143.
- (5) Harata, K.; Rao, C. T.; Pitha, J. *Carbohydr. Res.* **1993**, *247*, 83.
- (6) Soto Tellini, V. H.; Jover, A.; Galantini, L.; Mejjide, F.; Vázquez Tato, J. *Acta Crystallogr.* **2004**, *B60*, 204.
- (7) Miyauchi, M.; Kawaguchi, Y.; Harada, A. *J. Inclusion Phenom. Macrocyclic Chem.* **2004**, *50*, 57.
- (8) Miyauchi, M.; Takashima, Y.; Yamaguchi, H.; Harada, A. *J. Am. Chem. Soc.* **2005**, *127*, 2984.
- (9) Miyauchi, M.; Hoshino, T.; Yamaguchi, H.; Kamitori, S.; Harada, A. *J. Am. Chem. Soc.* **2005**, *127*, 2034.
- (10) Ramos Cabrer, P.; Alvarez-Parrilla, E.; Mejjide, F.; Seijas, J. A.; Rodríguez Nùñez, E.; Vázquez Tato, J. *Langmuir* **1999**, *15*, 5489.
- (11) Alvarez Parrilla, E.; Ramos Cabrer, P.; Singh, A. P.; Al-Soufi, W.; Mejjide, F.; Rodríguez Nùñez, E.; Vázquez Tato, J. *Supramol. Chem.* **2002**, *14*, 397.
- (12) Hoshino, T.; Miyauchi, M.; Kawaguchi, Y.; Yamaguchi, H.; Harada, A. *J. Am. Chem. Soc.* **2000**, *122*, 9876.
- (13) Liu, Y.; Wang, H.; Liang, P.; Zhang, H.-Y. *Angew. Chem., Int. Ed.* **2004**, *43*, 2690.
- (14) Liu, Y.; Li, L.; Zhang, H.-Y.; Zhao, Y.-L.; Wu, X. *Macromolecules* **2002**, *35*, 9934.
- (15) Alvarez Parrilla, E.; Ramos Cabrer, P.; Al-Soufi, W.; Mejjide, F.; Rodríguez Nùñez, E.; Vázquez Tato, J. *Angew. Chem., Int. Ed.* **2000**, *39*, 2856.
- (16) Soto, V. H.; Jover, A.; Carrazana, J.; Galantini, L.; Mejjide, F.; Vázquez Tato, J. *J. Am. Chem. Soc.* **2006**, *128*, 5728.

- (17) Hasegawa, Y.; Miyauchi, M.; Takashima, Y.; Yamaguchi, H.; Harada, A. *Macromolecules* **2005**, *38*, 3724.
- (18) Ohga, K.; Takashima, Y.; Takahashi, H.; Kawaguchi, Y.; Yamaguchi, H.; Harada, A. *Macromolecules* **2005**, *38*, 5897.
- (19) Breslow, R. *Pays-Bas* **1994**, *113*, 493.
- (20) Breslow, R.; Chung, S. *J. Am. Chem. Soc.* **1990**, *112*, 9659.
- (21) Breslow, R.; Halfon, S.; Zhang, B. *Tetrahedron* **1995**, *51*, 377.
- (22) Breslow, R.; Belvedere, S.; Gershell, L.; Leung, D. *Pure Appl. Chem.* **2000**, *72*, 333.
- (23) Zhang, B.; Breslow, R. *J. Am. Chem. Soc.* **1993**, *115*, 9353.
- (24) Carrazana, J.; Jover, A.; Meijide, F.; Soto, V. H.; Vázquez Tato, J. *J. Phys. Chem. B* **2005**, *109*, 9719.
- (25) Alvarez Parrilla, E.; Ramos Cabrer, P.; Pal Singh, A.; Al-Soufi, W.; Meijide, F.; Rodríguez Nùñez, E.; Vázquez Tato, J. *Supramol. Chem.* **2002**, *14*, 397.
- (26) Stabinger, H.; Kratky, O. *Makromol. Chem.* **1978**, *179*, 1655.
- (27) Glatter, O. In *Small Angle X-ray Scattering*; Glatter, O., Kratky, O., Eds.; Academic Press: London, 1982; p 119.
- (28) Orthaber, D.; Bergmann, A.; Glatter, O. *J. Appl. Crystallogr.* **2000**, *33*, 218.
- (29) Glatter, O. *J. Appl. Crystallogr.* **1977**, *10*, 415.
- (30) Durchschlag, H.; Zipper, P. *J. Com. Esp. Deterg.* **1995**, *26*, 275.
- (31) Berendsen, H. J. C.; van der Spoel, D.; van Drunen, R. *Comput. Phys. Commun.* **1995**, *91*, 43.
- (32) van Gunsteren, W. F.; Billeter, S.; Eising, A.; Hunenberger, P.; Kruger, P.; Mark, A. E.; Scott, W.; Tironi, I. *Biomolecular Simulations: The GROMOS96 Manual and User Guide*; BIOMOS bv: Groningen, 1996.
- (33) Lins, R. D.; Hunenberger, P. H. *J. Comput. Chem.* **2005**, *26*, 1400.
- (34) Oostenbrink, C.; Soares, T. A.; van der Vegt, N. F.; van Gunsteren, W. F. *Eur. Biophys. J.* **2005**, *34*, 273.
- (35) Oostenbrink, C.; Villa, A.; Mark, A. E.; van Gunsteren, W. F. *J. Comput. Chem.* **2004**, *25*, 1656.
- (36) Bayly, C. I.; Cieplak, P.; Cornell, W.; Kollman, P. A. *J. Phys. Chem.* **1993**, *97*, 10269.
- (37) Cornell, W. D.; Cieplak, P.; Bayly, C. I.; Kollmann, P. A. *J. Am. Chem. Soc.* **1993**, *115*, 9620.
- (38) Berendsen, H. J. C.; Grigera, J. R.; Straatsma, T. P. *J. Phys. Chem.* **1987**, *91*, 6269.
- (39) Evans, D. J.; Morriss, G. P. *Statistical Mechanics of Nonequilibrium Liquids*; Academic: London, 1990.
- (40) Hess, B.; Bekker, H.; Berendsen, H. J. C.; Fraaije, J. G. E. M. *J. Comput. Chem.* **1997**, *18*, 1463.
- (41) Essmann, U.; Perera, L.; Berkowitz, M. L.; Darden, T.; Lee, H.; Pedersen, L. G. *J. Chem. Phys.* **1995**, *103*, 8577.
- (42) Glatter, O. *Acta Phys. Austriaca* **1980**, *52*, 243.
- (43) Beveridge, D. L.; Di Capua, F. M. In *Computer Simulation of Biomolecular Systems*; van Gunsteren, W. F., Weiner, P. K., Eds.; ESCOM: Leiden, 1989; p 1.
- (44) Stellman, S. D.; Gans, P. J. *Macromolecules* **1972**, *5*, 516.
- (45) McGreevy, R. L. *J. Phys.: Condens. Matter* **2001**, *13*, R877.
- (46) Hamilton, J. A.; Sabesan, M. N. *Acta Crystallogr.* **1982**, *B38*, 3063.
- (47) Rekharsky, M. V.; Inoue, Y. *Chem. Rev.* **1998**, *98*, 1875.
- (48) Pedersen, J. S.; Schurtenberger, P. *Macromolecules* **1996**, *29*, 7602.
- (49) Pedersen, J. S.; Schurtenberger, P. *J. Polym. Sci., Part B: Polym. Phys* **2004**, *42*, 3081.
- (50) Jerke, G.; Pedersen, J. S.; Egelhaaf, S. U.; Schurtenberger, P. *Phys. Rev. E: Stat. Phys., Plasmas, Fluids, Relat. Interdiscip. Top.* **1997**, *56*, 5772.
- (51) Zhao, D.; Moore, J. S. *Org. Biomol. Chem.* **2003**, *1*, 3471.
- (52) Edwards, C. J. C.; Rigby, D.; Stepto, R. F. T.; Dodgson, K.; Semlyen, J. A. *Polymer* **1983**, *24*, 391.

MA070704U